The significant role of autophagy in the granular layer in normal skin differentiation and hair growth

Nagisa Yoshihara,[*1] Takashi Ueno,[*2] Atsushi Takagi,[*1] Juan Alejandro Oliva Trejo,[*2] Kunitaka Haruna,[*1] Yasushi Suga,[*1] Masaaki Komatsu,[*3] Keiji Tanaka,[*3] Shigaku Ikeda[*1]

[*1]Department of Dermatology and Allergology, Juntendo University Graduate School of Medicine, Tokyo, Japan

[*2]Division of Proteomics and Biomolecular Science, Research Support Center, Juntendo University Graduate School of Medicine, Tokyo, Japan

[*3]Protein Metabolism Project, Tokyo Metropolitan Institute of Medical Science, Tokyo, Japan

Corresponding author: Shigaku Ikeda, M.D., Ph.D., Department of Dermatology and Allergology, Juntendo University Graduate School of Medicine, 2-1-1 Hongo, Bunkyo-ku, Tokyo 113-8421

Tel: 81-3-5802-1089, Fax: 81-3-3813-9443, E-mail: ikeda@juntendo.ac.jp

Running title: Autophagy in the granular layer in normal skin differentiation and hair growth

Abstract

As a major intracellular degradation system, autophagy contributes to the maintenance of skin keratinocyte homeostasis. However, the precise role of autophagy in skin differentiation has not been fully investigated. To clarify whether autophagy plays a role in skin differentiation and maturation, autophagy-related gene 7 (Atg7)-deficient mice were generated. Atg7-deficient mice cannot survive for more than 24 hours after birth. Therefore, the skins of Atg7-deficient mice and wild-type mice (as a control) were grafted onto severe combined immunodeficient (SCID) mice. The resulting morphological and pathological changes were monitored for 28 days. Histopathological examination revealed acanthosis, hyperkeratosis, and abnormal hair growth in the skin grafts from the Atg7-deficient mice. Iimmune-density analysis of the skin grafts revealed reduced immunostaining of keratinization-related proteins, including loricrin, filaggrin, and involucrin, in the skin grafts from the Atg7-deficient mice. Furthermore, quantitative RT-PCR and Western blot analyses revealed the reduced expression of these three keratinization-related proteins in the skin grafts from the Atg7-deficient mice. Morphometric analysis using electron microscopy further revealed a reduction in the number and diameter of the keratohyalin and trichohyaline granules in these skin grafts. The differences were maintained for at least 1 month after transplantation. These results show that autophagy has a significant role in epidermal keratinization and hair growth until a certain stage of maturation.

Key words: autophagy・keratinocyte・keratinization・hair growth・keratohyalin granule・keratinization-related proteins

Introduction

Autophagy is a process in which cellular constituents are transported to and degraded in the lysosome. In contrast to the ubiquitin-proteasome system, which is another cellular degradative process that has strict selectivity, autophagy non-selectively degrades all the proteins and organelles within the space surrounded by the isolation membrane of the autophagosome in a process referred to as bulk degradation [4, 11, 24, 25]. Autophagy is an efficient cell survival system because the amino acids and other degradation products produced by autophagy are returned to or recycled in the cytoplasm [4, 24, 25, 26]. It has been recently demonstrated that autophagy participates in a wide range of cell survival processes, including innate immunity, antigen presentation, and anti-aging, as well as cellular protection from various disorders, such as neurodegenerative diseases [9, 16, 17], cancer [22], and others [5, 8, 14, 23].

There have been few reports related to the mechanism of autophagy in the skin, and the role of autophagy in the skin has not yet been clarified in detail [27]. Although autophagy-deficient mice are born normal with features similar to their wild-type littermates, they tend to weigh slightly less compared with wild-type mice [15, 18] and die within 24 hours after birth. Therefore, while it is necessary to observe their skin over time in order to obtain a precise understanding of whether autophagy is required for skin differentiation, it is not possible to assess the contribution of autophagy to skin development in these knockout mice [15, 18] due to their short lifespan. To address this problem, we transplanted the skin from newborn autophagy-deficient mice onto the backs of severe combined immunodeficient (SCID) mice and observed the maturation of the skin grafts over time. Furthermore, we sought to compare the findings in the skin grafts from the knockout mice with skin grafts from wild-type mice.

Materials and Methods

Animals

Autophagy-related gene 7 (Atg7)-deficient mice were generated and bred as described previously [15]. All the wild-type and Atg7-deficient mice were maintained on a C57BL/6J genetic background. The genotypes of the neonates were determined via PCR analysis of the tail DNA using two primers (Primer 1: 5′-TGGCTGCTACTTCTGCAATGATGT-3′ and primer 2: 5′-TTAGCACAGGGAACAGCGCTCATGG-3′). The skin grafts taken from the 7 Atg7-deficient mice and the 7 control wild-type littermates were then transplanted onto the backs of the SCID mice and examined

over time. The SCID mice maintained on a CB17/Icr genetic background were purchased from the Charles River Laboratory Japan (Yokohama, Japan). All the mice were maintained in an environmentally controlled room (illuminated between 08:00 and 20:00) and were fed a pelleted laboratory diet, with tap water available ad libitum. All the animal experiments were conducted with prior approval from the Ethics Review Committee for Animal Experimentation of Juntendo University.

Skin transplantation

All the newborn Atg7-deficient mice were euthanized, and 1-cm-diameter circular pieces of their dorsal skin were excised and transplanted onto the backs of the SCID mice. As a control, the skin of the wild-type littermates was transplanted in a similar manner. On the 7^{th}, 14^{th}, and 28^{th} day after the transplantation, the skin grafts from the two groups were excised and compared with macroscopic, histopathological (light and electron microscopic), and immunohistochemical analyses.

Morphological analysis

On the 7^{th}, 14^{th}, and 28^{th} day after transplantation, the skin grafts from the Atg7-deficient and wild-type mice were collected and immediately fixed in neutral buffered formalin for examination by light microscopy. To prepare the sections for electron microscopy, the skin grafts were fixed in a 2.5% glutaraldehyde solution. Using hematoxylin and eosin (H&E)-stained specimens, the epidermal thicknesses were measured, and the mean ± standard deviation was calculated. The thicknesses of the outer root sheathes were also measured, and the mean ± standard deviation was calculated.

Immunohistochemical staining and immune-density analysis

All the specimens for immunohistochemistry were fixed in formalin and then embedded in paraffin. The sections prepared from these specimens were subjected to immunohistochemical staining with polyclonal antibodies against LC3 (ab48394, Abcam, Cambridge, MA, USA), loricrin (Covance, Richmond, CA, USA), filaggrin (ab24584, Abcam, Cambridge, MA, USA), and involucrin (Covance, Richmond, CA, USA).

LC3 was used to assess the functional state of the autophagy. The keratinization-related proteins examined in this study, including loricrin, filaggrin, and involucrin, are expressed in the uppermost granular

layer, the granular layer, and the upper spinous layer, respectively. Autophagy is involved in programmed cell death [28]. Therefore, it was considered highly likely that autophagy would act strongly around the granular layer of the skin where the cells are denucleated. The 3 keratinization-related proteins were used to investigate at which level autophagy acted around the granular layer.

Immunostaining was performed according to the standard linked streptavidin-biotin (LSAB) method. The reaction products were developed for color with diaminobenzidine and counterstained with hematoxylin. After immunostaining the grafts, the staining intensities of LC3, loricrin, filaggrin, and involucrin expression were quantified using the KS-400 version 4.0 image analysis system (KS-400; Carl Zeiss Vision, Munich, Germany). The epidermal layer intensities were measured in 3 randomly selected fields for each section, and the analyses were performed by two investigators in a blinded manner. Microscopic images of each section were imported into the KS-400 image software, in which brown-stained areas that represented positive immunostaining were converted into a 255-graded gray scale. In the analysis system, 0 indicated the highest density (strongest immunoreactivity), and 255 indicated the lowest density (lowest immunoreactivity). Each value obtained was subtracted from 255, and this difference (Δ gray-scale intensity) was used for the quantitative analysis of the immunointensity.

Quantitative real time (RT)-PCR

The skin grafts were excised from the backs of the host SCID mice and incubated immediately with RNAlater (Qiagen, Venlo, Netherlands). Total RNA was isolated with the use of TRIzol (Life Technologies Co., Carlsbad, CA, USA). Reverse transcription was performed with 1 μg of RNA using a high capacity cDNA reverse transcription kit (Applied Biosystems, CA, USA). The specific mRNAs were amplified with a SYBR Green PCR Master Mix (Applied Biosystems) in an ABI PRISM 7500 thermal cycler (Applied Biosystems). The relative amounts of mRNA were calculated with β-actin mRNA as the invariant control.

Epidermal protein extraction and Western blot analysis

On the 7th day after the transplantation, the skin grafts from the wild-type and Atg7-deficient mice were excised from the backs of the host SCID mice and suspended in a buffer containing 5 mM Tes-NaOH (pH 7.4), 0.3 M sucrose, and proteinase inhibitors (Complete Mini, Roche Diagnostics Co., IN,

USA). The suspension was extensively homogenized with a motor-driven glass/Teflon homogenizer. The resultant homogenate was mixed with SDS-PAGE sample buffer and incubated at 100°C for 5 min. The Western blot analysis was performed as described previously [13] using rabbit antibodies to filaggrin, involucrin, and loricrin (Covance Inc., NJ, USA). Antibodies to Atg7 and LC3 were prepared as described previously [15]. Actin was used as the loading control.

Electron microscopy and morphometric analysis

Transmission electron microscopy was performed to observe the epidermal morphology and to measure the number and diameter of the keratohyalin and trichohyaline granules. Scanning electron microscopy was primarily performed on the surface of the hair shafts.

For the transmission electron microscopy, the skin grafts were fixed in Karnovsky's fixative and embedded in epoxy resin according to the standard procedures. Ultrathin sections (approximately 0.07 μm) were prepared, stained with uranyl acetate and lead citrate, and observed with an HT7700 (HITACHI, Tokyo, Japan) transmission electron microscope at 100 kV. Photographs were taken with the microscope's built-in camera. The number of keratohyalin granules in the most superficial granular layer and trichohyaline granules in the inner root sheath layer of the anagen hair were measured in 5 randomly selected fields for each section on 700 images, and the mean numbers were compared.

For the scanning electron microscopy observations, the hair shafts were dehydrated in 100% ethanol. After coating with platinum, the samples were examined with an HT4800 scanning electron microscope (Hitachi, Japan) at 15 kV.

Statistics

Significant differences were calculated using the Wilcoxon test, and $P < 0.05$ was set as the level of significance.

Results

Macroscopic findings

On the 7th day after the transplantation, the skin grafts from both the Atg7-deficient and

wild-type mice were well attached (Fig. 1a, 1d). On the 14th day after the transplantation, the donor-derived black hair was observed on both skin grafts (Fig. 1b, 1e). On the 28th day after the transplantation, both the skin grafts were covered with black hair (Fig. 1c, 1f). Thus, at first glance, the hair on the grafts from the two groups appeared similar to the unaided eye. We then closely observed the skin grafts at both the light and electron microscopic levels.

Histopathological findings of the epidermis

On the 7th day after the transplantation, the skin grafts from the Atg7-deficient mice exhibited acanthosis and hyperkeratosis (Fig. 2a, 2d). Similar changes were observed on the 14th and 28th days, although these abnormalities tended to attenuate gradually (Fig. 2b, 2c, 2e, and 2f; and Table 1). On the 7th day after the transplantation, the epidermal thickness was significantly greater ($P = 0.033$, n = 7) in the skin grafts from the Atg7-deficient mice (1753.2 ± 120.3 μm) compared with the control skin grafts (1445.7 ± 99.1 μm). On the 14th and 28th days after the transplantation, the epidermal thickness was also found to be significantly greater ($P = 0.022$ and $P = 0.008$, respectively, n = 7) in the skin grafts from the Atg7-deficient mice (1535.6 ± 217.0 μm and 526.0 ± 147.8 μm, respectively) compared with the wild-type mice (1037.7 ± 50.4 μm and 353.3 ± 51.6 μm, respectively). Thus, the skin thickness of the grafts from the Atg7-deficient mice was significantly increased compared with that from the wild-type mice at all the stages up to 28 days after the transplantation.

Histopathological findings from the hair

The skin grafts from the Atg7-deficient mice displayed significantly slower hair growth compared with the control group. On the 7th day after the transplantation, a few immature hair bulbs were noted in the skin of the Atg7-deficient mice, whereas numerous mature hair bulbs containing melanocytes were observed in the control. In addition, the thickness of the outer root sheath tended to be greater in the skin grafts from the Atg7-deficient mice compared with the skin grafts from the control mice (Fig. 2g, 2j, 2n, 2n', 2o, 2o').

On the 14th day after the transplantation, the hair shafts were observed in the control group, but fewer were noted in the skin grafts from the Atg7-deficient mice (Fig. 2h, 2k). The thickness of the outer

root sheath was significantly greater ($P < 0.001$) in the skin grafts from the Atg7-deficient mice (921.8 ± 60.8 μm) compared with the skin grafts from the control mice (585.4 ± 14.9 μm) (Table 1).

On the 28th day after the transplantation, many follicles in the anagen stage were primarily observed in both grafts. Impaired hair growth was no longer observed (Fig. 2i, 2m). The thickness of the outer root sheath was also significantly greater ($P = 0.008$, n = 7) in the skin grafts from the Atg7-deficient mice (823.8 ± 168.5 μm) compared with the skin grafts from the control mice (636.8 ± 82.0 μm) (Table 1).

Immunohistochemical findings and immune-density analysis

Immunostaining for the keratinization-related proteins loricrin, filaggrin, and involucrin revealed a significant reduction in the expression of these proteins in the Atg7-deficient mice compared with the wild-type mice (Fig. 3, day 14). Loricrin staining was strongly positive immediately below the stratum corneum in the control skin grafts. In contrast, loricrin staining was only weakly positive over a wide area in the skin grafts from the Atg7-deficient mice and extended from the upper spinous layer to immediately below the stratum corneum (Fig. 3a, 3b). The average Δ gray-scale intensity of the epidermis area was significantly lower ($P = 0.03$, n = 7) in the grafts from the Atg7-deficient mice compared with the grafts from the control mice (Fig. 3c). Immunohistological staining for filaggrin revealed that a part of the granular layer in the control skin grafts was stained, but this region was only slightly stained in the skin grafts from the Atg7-deficient mice (Fig. 3d, 3e). The average Δ gray-scale intensity in the granular layer was significantly lower ($P = 0.03$, n = 7) in the grafts from the Atg7-deficient mice compared with the grafts from the control mice (Fig. 3f). The positively stained area in the granular layer was significantly smaller ($P = 0.006$) in the grafts from the Atg7-deficient mice (8.2 ± 8.2%) compared with the grafts from the control mice (36.5 ± 24.5%). Involucrin staining was positive in all the epidermal layers in both of the groups (Fig. 3g, 3h). The average Δ gray-scale intensity of the epidermis was significantly lower ($P = 0.003$, n = 7) in the grafts from the Atg7-deficient mice compared with the grafts from the control mice (Fig. 3i).

Similarly, LC3 staining was moderately positive in the skin grafts from the control mice but was only weakly positive in the skin grafts from the Atg7-deficient mice, with significant differences (Fig. 3j, 3k, 3l).

Thus, the expression of the keratinization-related proteins, including loricrin, filaggrin and involucrin, as well as the autophagy marker LC3, was reduced in the skin grafts from the Atg7-deficient mice compared with the skin grafts from the wild-type mice. These staining differences between the skin grafts from the Atg7-deficient and the wild-type mice tended to gradually decrease on the 28th day after transplantation (data not shown).

Quantitative RT-PCR analysis

The quantitative RT-PCR analysis revealed that the expression of filaggrin and loricrin was significantly reduced in the skin grafts from the Atg7-deficient mice (n = 3) compared with the skin grafts from the wild-type mice (n = 3). The expression of involucrin tended to be lower in the skin grafts from the Atg7-deficient mice compared with the skin grafts from the wild-type mice (Fig. 4).

Western blot analysis

Western blot analysis was performed with the skin graft homogenate from the wild-type and Atg7-deficient mice on the 7th day after the transplantation (Fig. 5). First, Atg7 deficiency and the resulting lack of LC3-II were clearly shown in the skin graft homogenate from the Atg7-deficient mice. The faint signals of Atg7 and LC3-II seen in the Atg7-deficient grafts most likely derive from the SCID mouse tissues associated with the graft that could not be removed when the grafts were excised. The data revealed that the levels of loricrin, involucrin and filaggrin were significantly lower in the skin grafts from the Atg7-deficient mice (n = 2) compared with the skin grafts from the wild-type mice (n = 2).

Transmission electron microscopic findings and morphometric analysis

Figure 6 shows the electron micrographs of the skin grafts from the Atg7-deficient and wild-type mice. The morphometry indicated that the number and maximum diameter of the keratohyalin granules in a 50 μm^2 (10 $\times$ 5 μm) area were 9.4 $\pm$ 1.1 and 1.4 $\pm$ 0.8 μm, respectively, in the Atg7-deficient grafts and 13.5 $\pm$ 1.9 and 2.9 $\pm$ 0.9 μm, respectively, in the control skin grafts (Fig. 6a, 6d, 6g, 6j, day 7). Overall, the skin grafts from the Atg7-deficient mice showed a reduction in the number and diameter of

keratohyalin granules, with significant differences ($P < 0.05$) compared with the skin grafts from the control mice. Similar differences were also observed on the 14th (Fig. 6b, 6e, 6h, 6k) and 28th (Fig. 6c, 6f, 6i, 6l) days after the transplantation. The number and maximum diameter of the granules in the skin grafts from the Atg7-deficient mice were 7.5 ± 1.0 and 1.3 ± 0.1 μm, respectively, on the 14th day and 7.4 ± 1.7 and 1.5 ± 0.5 μm, respectively, on the 28th day, whereas these values for the skin grafts from the control mice were 12.7 ± 1.3 and 2.7 ± 0.3 μm, respectively, on the 14th day and 10.4 ± 1.2 and 2.4 ± 0.3 μm, respectively, on the 28th day. Although the abnormalities tended to attenuate over time after the transplantation, significant differences between the skin grafts from the Atg7-deficient mice and the wild-type mice were still observed after 28 days.

Electron microscopic findings from the hair

In the scanning electron micrographs, the hair in the skin grafts from the Atg7-deficient mice exhibited an extremely irregular cuticle that was similar to a horsetail in configuration; in contrast, the hair in the skin grafts from the control mice displayed normal cuticles in a regular pattern (Fig. 7a, 7c). The diameter of the hairs in the Atg7-deficient mice was reduced compared with the control. This anomaly was observed until 6 weeks after the transplantation. The spacing between the hairs was wider in the skin grafts from the Atg7-deficient mice compared with the control. The number and maximum diameter of the trichohyaline granules was significantly reduced in the skin grafts from the Atg7-deficient mice compared with the skin grafts from the control mice (Fig. 7b, 7d, Table 1).

Discussion

Autophagy has been reported to be induced in keratinocytes and to play a role in differentiation in vitro [1, 6, 7, 10, 19, 32]. Atg7-deficient mice are born normal, similar to their wild-type littermates, which suggests that autophagy deficiency does not affect the skin morphogenesis of neonates [15, 18]. However, these two reports did not carefully investigate the morphology of either the epidermis or the hair follicle. It would be interesting to investigate the epidermal phenotype in Atg7-null neonatal mice. Because Atg7-deficient mice die within 24 hours after birth, the role of autophagy in the differentiation and maturation into adult skin over an extended period of time is not known.

The SCID mouse is a useful animal model for the analysis of transplanted skin grafts in the absence of an immune rejection by the host. Studies using this experimental model have been widely conducted, and the validity of this model for understanding the pathological changes in skin grafts transplanted from genetically modified mice and humans has been well documented [2, 3]. We transplanted skin grafts from the Atg7-deficient mice onto the SCID mice. This model allowed us to observe the skin grafts for an extended period of time (approximately 1 month) to investigate whether autophagy is required for skin differentiation.

Our experimental plan was to first confirm an autophagy deficiency in the skin grafts from the Atg7-deficient mice using LC3 as a marker. As a specific component of the autophagosome membrane, LC3 is recruited both inside and outside of the isolation membrane. For this recruitment to the autophagosome, proLC3 that is synthesized in the cytoplasm is converted by Atg4B to LC3-I; LC3-I is then conjugated with phosphatidylethanolamine to generate LC3-II by a ubiquitylation-like modification catalyzed by Atg7 and Atg3 [11]. The skin grafts from the Atg7-deficient mice showed LC3 immunostaining, but the intensity was significantly weaker compared with the control skin grafts (Fig. 3). The weak LC3-staining in the skin of the Atg7-deficient mice is considered to represent LC3-I that has not been converted to LC3-II. This was further confirmed in the Western blot analysis (Fig. 5). Diffuse LC3 staining throughout the entire epidermis is consistent with the data of Shi JH et al. [12].

Our histopathological examination revealed acanthosis and hyperkeratosis in the skin grafts from the Atg7-deficient mice. The morphometric analysis via electron-microscopic observation revealed a reduction in the number and diameter of the keratohyalin granules (Fig. 6). These abnormalities continued but tended to attenuate over the following 28 days. Autophagy has been reported to be constitutively active in the epidermis, but autophagy is not essential for the function of the epidermal barrier, as demonstrated by experiments with keratin 14 (K14)-Cre-Atg7 F/F mice [30, 31]. These results are consistent with our results that were obtained at a later stage after the transplantation (day 28). It should be emphasized that this detailed assessment of the changes over time has unveiled an autophagy requirement for the differentiation of smooth skin at earlier stages. In addition to incomplete epidermal keratinization (Figs. 2 and 3), the skin grafts from the Atg7-deficient mice revealed a hair-growth disorder, which suggests that autophagy is also necessary for proper hair growth (Fig. 4). The skin grafts from the Atg7-deficient mice exhibited a thickened outer root sheath and a reduction in the number and maximum

diameter of the trichohyaline granules. These results suggest that autophagy controls cornification in the hair and the epidermis. However, these abnormalities were not actually observed in the K14-cre-loxP-mediated Atg7 knockout mice [30] but were considered likely to occur because the Atg7 deletion was specifically introduced in the epidermal keratinocytes of these mice. In contrast, full-skin grafts that included the lower epidermis, which is also autophagy deficient, were transplanted onto the SCID mice in our model. Thus, the hair disorder indicated by an abnormal cuticle pattern is quite noteworthy in the Atg7-deficient grafts under our experimental regimen.

In accordance with these findings, we found that the immunostaining of filaggrin, which is enriched in the granular layer, was weaker in the skin grafts from the Atg7-deficient mice. Subtle and diffuse staining for loricrin and involucrin was also recognized over a wider epidermal area in the skin grafts from the Atg7-deficient mice compared with the control skin grafts. Involucrin and loricrin are present in the cornified layer of the epidermis, as is caspase 14, which plays an important role in terminal epidermal differentiation [21, 29]. These abnormalities were most prominent on the 14^{th} day after the transplantation and tended to diminish gradually thereafter. To confirm the reduction of the keratinization-related proteins, we conducted Western blot and quantitative RT-PCR analyses. These results showed the reduced expression of keratinization-related proteins at both the transcriptional and translational levels, which further supports the immunohistochemical findings. These results, along with the decreased number of keratohyalin granules (Fig. 6), suggest that the autophagy deficiency is more severe in the granular layer compared with the other layers of the epidermis. Autophagic degradation is necessary for cellular remodeling during differentiation [24, 25]. The reduction in the number of keratohyalin granules and the decreased expression of filaggrin are indicative of the retardation of granular layer differentiation in the autophagy-deficient grafts.

In summary, our findings suggest that autophagy is not essential for skin formation itself, but is important for terminal epidermal keratinization and hair growth in the earlier stages of differentiation. In view of these characteristics of autophagy-deficient skin, it is important to investigate whether autophagy deficiency elicits a more severe outcome in certain skin diseases that involve barrier dysfunction, such as atopic dermatitis [20]. Further studies exploring the relationship between autophagy impairment and the pathogenesis of barrier dysfunction diseases are necessary to develop novel therapeutics in the near future.

Acknowledgments

We are grateful to Dr. Norihito Tada, Dr. Takatoshi Kuhara, and the staff of the Atopy Research Center for breeding the Atg7-deficient mice. We thank Mr. Atsushi Furuhata and Ms. Yuko Kojima of the Laboratory of Biomedical Imaging Research, and Dr. Masato Koike and Mr. Mitsutaka Yoshida of the Laboratory of Ultrastructure Research and the Laboratory of Molecular and Biochemical Research, Research Support Center, Juntendo University Graduate School of Medicine, Tokyo, Japan, for technical assistance. This work was supported, in part, by the "Research on Measures for Intractable Diseases" Project matching fund subsidy (H23-028) from the Ministry of Health, Labor, and Welfare, Japan (AT, SI), a Grant-in-aid for Scientific Research on Priority Areas (18076005 to MK, TU), and a Research Grant from the Takeda Science Foundation (TU).

Conflict of interest

The authors declare that they have no conflicts of interest.

References

1. Aymard E, Barruche V, Naves T et al (2011) Autophagy in human keratinocytes: an early step of the differentiation? Exp Dermatol 20:263–268

2. Boehncke WH, Schön MP (2007) Animal models of psoriasis. Clin Dermatol. 25:596–605

3. Candi E, Schmidt R, Melino G (2005) The cornified envelope: a model of cell death in the skin. Nat Rev Mol Cell Bio 6:328–340

4. Choi AM, Ryter SW, Levine B (2013) Autophagy in human health and disease. N Engl J Med 368:651–662

5. Ebato C, Uchida T, Arakawa M et al (2008) Autophagy is important in islet homeostasis and compensatory increase of beta cell mass in response to high-fat diet. Cell Metab 8:325–332

6. Eckhart L, Declercq W, Ban J et al (2000) Terminal differentiation of human keratinocytes and stratum corneum formation is associated with caspase-14 activation. J Invest Dermatol 115:1148–1151

7. Elias PM (2005) Statum corneum defensive functions: an integrated view. J Invest Dermatol 125:183–300

8. Fujishima Y, Nishiumi S, Masuda A et al (2011) Autophagy in the intestinal epithelium reduces endotoxin-induced inflammatory responses by inhibiting NF-KappaB activation. Arch Biochem Biophys 506:223–235

9. Hara T, Nakamura K, Matsui M et al (2006) Suppression of basal autophagy in neural cells causes neurodegenerative disease in mice. Nature 441:885–889

10. Haruna K, Suga Y, Muramatsu S et al (2008) Differentiation-specific expression and localization of an autophagosomal marker protein (LC3) in human keratinocytes. J Dermatol Sci 52:213–215

11. He C, Klionsky DJ (2009) Regulation mechanisms and signaling pathways of autophagy. Annu Rev Genet 43:67–93

12. Shi JH, Hu DH, Zang ZF et al (2012) Reduced expression of microtubule-associated protein1 light chain 3 in hypertrophic scar. Arch Dermatol Res 304:209–215

13. Juanes S, Epp N, Latzko S et al. (2009) Development of an ichthyosiform phenotype in Alox12b-deficient mouse skin transplants. J Invest Dermatol 129:1429–1436

14. Jung HS, Chung KW, Won Kin J et al (2008) Loss of autophagy diminishes pancreatic beta cell mass and function with resultant hyperglycemia. Cell Matab 8:318–324

15. Komatsu M, Waguri S, Ueno T et al (2005) Impairment of starvation- induced and constitutive autophagy in Atg-7 deficient mice. J Cell Biol 169:425–434

16. Komatsu M, Waguri S, Chiba T et al (2006) Loss of autophagy in the central nervous system causes neurodegeneration in mice. Nature 441:880–884

17. Komatsu M, Waguri S, Koike M et al. (2007) Homeostatic levels of p62 control cytoplasmic inclusion body formation in autophagy- deficient mice. Cell 131:1149–1163

18. Kuma A, Hatano M, Matsui M et al (2004) The role of autophagy during the early neonatal starvation period. Nature 432:1032–1036

19. Lee HM, Shin DM, Yuk JM et al (2011) Autophagy negatively regulates keratinocyte inflammatory response via scaffolding protein p62/SQSTM1. J Immunol 186:1248–1258.
20. Leung DY (2013) New insights into atopic dermatitis: role of skin barrier and immune dysregulation. Allergol Int. 62:151-161.

21. Lippens S, Kockx M, Knaapen M et al (2000) Epidermal differentiation does not involve the pro-apoptotic executioner caspases, but is associated with caspase-14 induction and processing. Cell Death Differ 7:1218–1224

22. Takamura A, Komatsu M, Hara T, et al. (2011) Autophagy-deficient mice develop multiple liver tumors. Genes Dev 25:795-800.

23. Masiero E, Agatea L, Mammucari C et al. (2009) Autophagy is required to maintain muscle mass. Cell Metab 10:507–515

24. Mizushima N, Komatsu M (2011) Autophagy: renovation of cells and tissues. Cell 147:728–741

25. Mizushima N, Levine B (2010) Autophagy in mammalian development and differentiation. Nat Cell Biol 12:823–830

26. Mizushima N, Yoshimori T, Levine B (2010) Methods in mammalian autophagy research. Cell 140:313–326

27. Mizushima N, Yamamoto A, Matsui M et al (2004) In vivo analysis of autophagy in response to nutrient starvation using transgenic mice expressing a fluorescent autophagosome marker. Mol Bio Cell 15:1101–1111

28. Nikoletopoulou V, Markaki M, Palikaras K, Tavernarakis N (2013) Crosstalk between apoptosis, necrosis and autophagy. Biochim Biophys Acta. 1833:3448-3459

29. Rendl M, Ban J, Mrass P et al (2002) Caspase-14 expression by epidermal keratinocytes is regulated by retinoids in a differentiation-associated manner. J Invest Dermatol 119:1150–1155

30. Rossiter H, Konig U, Barresi C et al (2013) Epidermal keratinocytes form a functional skin barrier in the absence of Atg7 dependent autophagy. J Dermatol Sci 71:67–75

31. Sukseree S, Mildner M, Rossiter H et al (2012) Autophagy in thymic epithelium is dispensable for the development of self-tolerance in a novel mouse model. PLoS ONE 7:e389

32. Wang RC, Levine B (2011) Calcipotriol induces autophagy in HeLa cells and keratinocytes. J Invest Dermatol 131:990–993

Table 1 Comparison between the skin grafts from the Atg7-deficient and wild-type mice using morphometric analysis

	Atg7 KO (n = 7)	control (n = 7)	*P* value
Epidermal thickness (μm)			
Day 7	1753.2 ± 120.3	1445.7± 99.1	0.033
Day 14	1535.6 ± 217.0	1037.7 ± 50.4	0.022
Day 28	526.0 ± 147.8	353.3 ± 51.6	0.008
Number of keratohyaline granules (/50 μm^2)			
Day 7	9.4±1.1	13.5±1.9	0.014
Day 14	7.5±1.0	12.7±1.3	0.010
Day 28	7.4±1.7	10.4±1.2	<0.001
Maximum diameter of keratohyaline granules (μm)			
Day 7	1.4 ± 0.8	2.9 ±0.9	0.026
Day 14	1.3 ± 0.1	2.7 ±0.3	0.009
Day 28	1.5 ± 0.5	2.4 ±0.3	0.015
Thickness of outer root sheath (μm)			
Day 7	1049.6 ±155.2	620.4 ±46.4	0.030
Day 14	921.8 ±60.8	585.4 ±14.9	<0.001
Day 28	823.8 ±168.5	636.8 ±82.0	0.008
Number of trichohyaline granules (/50 μm^2)			
Day 7	8.3±1.0	10.5±1.3	0.038
Day 14	10.0±0.8	12.8±0.5	0.026
Day 28	6.8±1.0	11.5±1.7	0.028
Maximum diameter of trichohyaline granules (μm)	1.8±0.3	2.5±0.5	0.033
Day 7	2.0 ±0.1	2.6 ±0.8	0.014
Day 14	2.1±0.4	3.0±0.5	0.033
Day 28			

The data are expressed as the means ± S.D.

Figure Captions

Fig. 1 Gross morphology

The gross morphology of the skin from the Atg7-deficient and wild-type mice grafted onto the SCID mice on the 7^{th}, 14^{th}, and 28^{th} day after the transplantation. The hair of the two groups appears similar on day 28.

Fig. 2 Histopathological findings from the epidermis and hair (hematoxylin and eosin)

The control skin grafts were normal (d, e, and f). In contrast, the skin grafts from the Atg7-deficient mice exhibited acanthosis and severe hyperkeratosis (a, b, and c). These abnormalities tended to attenuate after the transplantation. The lower 6 panels (g, h, i, j, k, and m) show the difference in the hair between the skin grafts from the control mice and those from the Atg7-deficient mice. In the skin grafts from the Atg7-deficient mice, impaired hair growth and outer root sheath thickness were observed (g and i). The asterisk (*) indicates the immature hair bulb. The right panels (n, n', o, o') are longitudinal sections of the entire hair follicle on day 7. Scale bars (a–m) = 50 μm, (n, o) = 100 μm, and (n', o') = 200 μm.

Fig. 3 Immunohistochemical findings and immune-density analysis

The sections of the grafted skin from the control (left panel) and Atg7-deficient mice (right panel) were immunostained for the keratinization-related proteins and autophagy-related markers. The staining for loricrin (a, b), filaggrin (d, e), involucrin (g, h), and LC3 (j, k) was more intense in the skin grafts from

the control mice compared with those from the Atg7-deficient mice. Scale bars (a–j) = 50 μm. The regions marked by the outlined arrows (control wild-type grafts) and the regions marked by the filled arrows (Atg7-deficient grafts) were quantified using the KS-400 version 4.0 image analysis system. The average Δ gray-scale intensities for loricrin, filaggrin, involucrin, and LC3 within the entire epidermis were lower in the skin grafts from the Atg7-deficient mice compared with the control skin grafts (c, f, i, l), $*p < 0.05$.

Fig. 4 Quantitative RT-PCR analysis

The quantitative RT-PCR analysis revealed that the expression of filaggrin and loricrin was significantly reduced in the skin grafts from the Atg7-deficient mice compared with the skin grafts from the wild-type mice. The expression of involucrin tended to be lower in the skin grafts from the Atg7-deficient mice compared with the skin grafts from the wild-type mice, $*p< 0.05$.

Fig. 5 Western blot analysis

Skin grafts from the wild-type (WT) and Atg7-deficient (KO) mice on the 7^{th} day after transplantation were processed to prepare a total homogenate as described in the Materials and Methods section. The homogenate was separated in either 10% or 12.5% SDS-PAGE gels and subjected to Western blotting using anti-bodies to Atg7, involucrin, loricrin, filaggrin, actin, and LC3. The levels of loricrin, involucrin

and filaggrin were lower in the skin grafts from the Atg7-deficient mice compared with the skin grafts from the wild-type mice. The data are representative of more than three separate experiments.

Fig. 6 Transmission electron microscopic findings and morphometric analysis

Transmission electron micrographs (a–l) showing a reduced number and diameter of keratohyalin granules in the skin grafts from the Atg7-deficient mice compared with the skin grafts from the control. Scale bars (a–l) = 10.0 μm. The morphometric data comparing the size and number of trichohyaline granules in the skin grafts between the control and Atg7-deficient mice (m and n, $*p < 0.05$).

Fig. 7 Electron microscopic findings from the hair

The skin grafts from the control mice have a normal cuticle in a regular pattern, and the skin grafts from the Atg7-deficient mice have an irregular cuticle (a and c). Transmission electron micrographs (b and d) showing the reduced number and diameter of the trichohyaline granules in the skin grafts from the Atg7-deficient mice compared with the skin grafts from the control mice. Scale bars (a, c) = 50 μm; (b, d) = 5.0 μm.

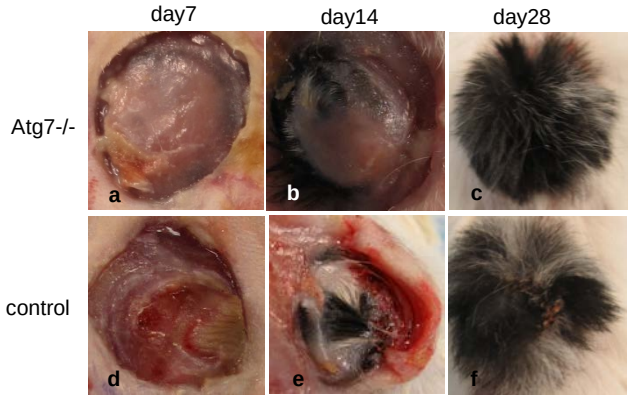
day7
day14
day28
Atg7-/-
control
a
b
c
d
e
f

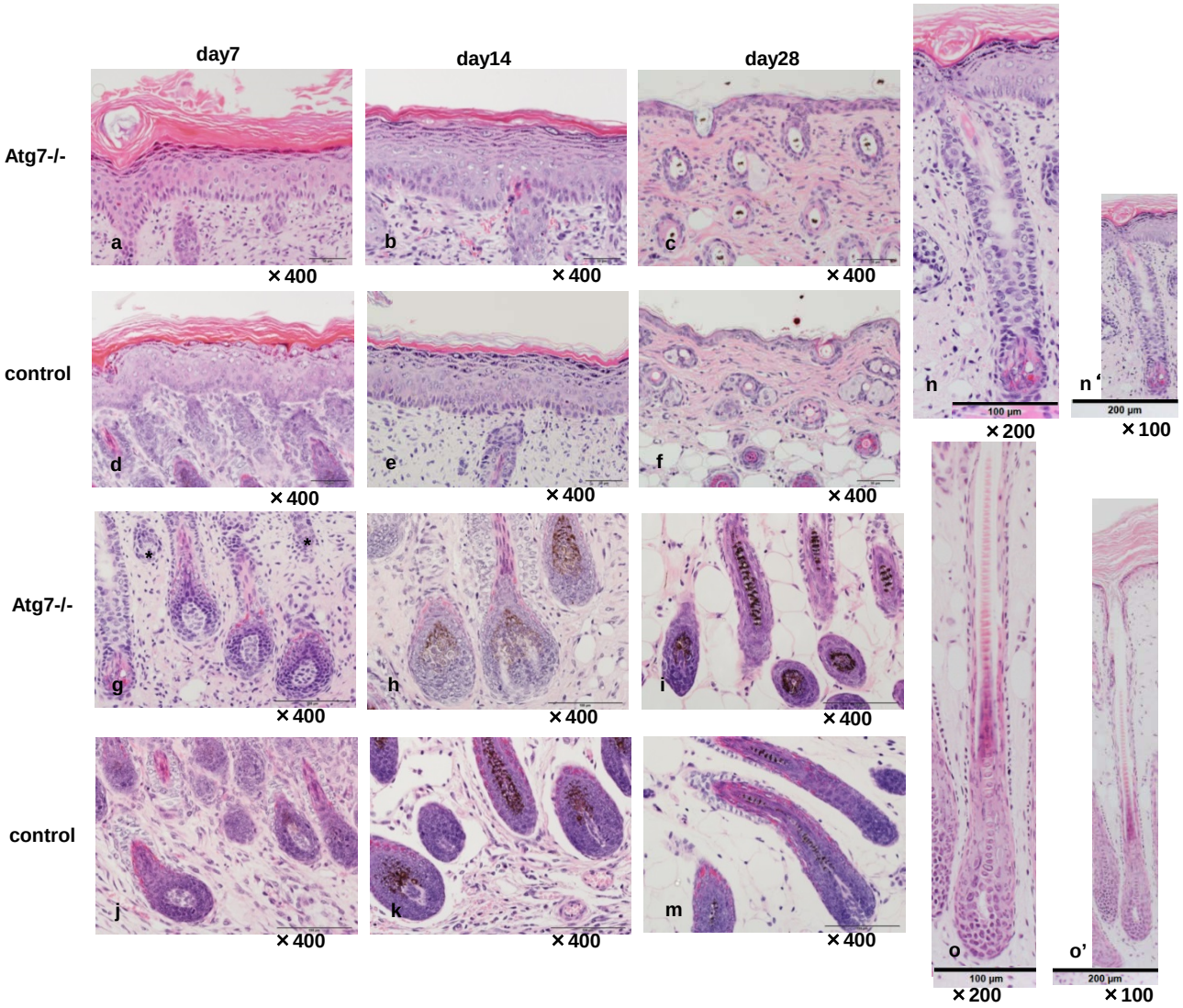
day7
day14
day28
Atg7-/-
control
Atg7-/-
control
a
b
c
d
e
f
g
h
i
j
k
m
n
n'
o
o'
×400
×200
×100
100 μm
200 μm

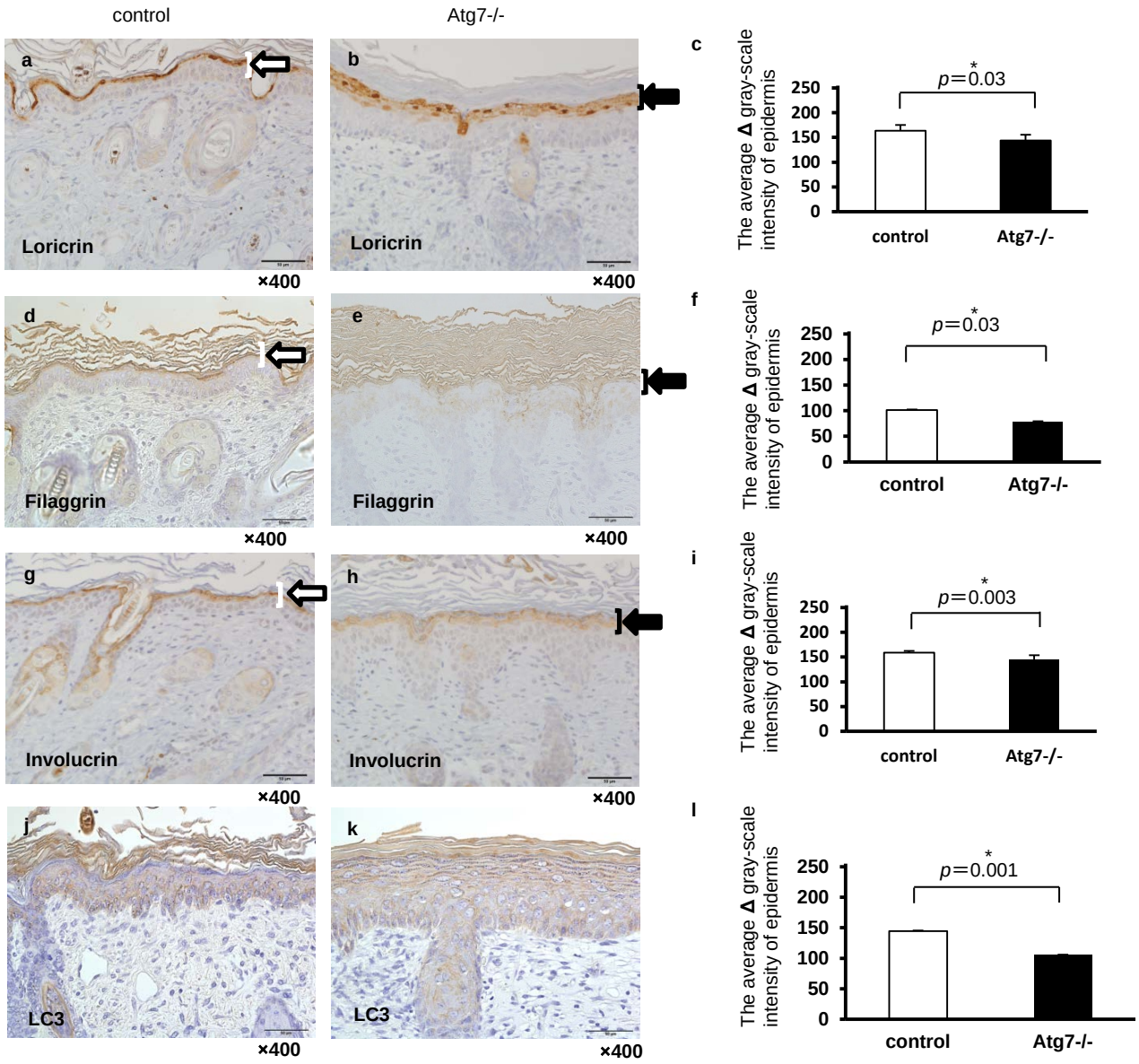
control
Atg7-/-
a
Loricrin
×400
b
Loricrin
×400
c
The average Δ gray-scale intensity of epidermis
*
p=0.03
250
200
150
100
50
0
control
Atg7-/-
d
Filaggrin
×400
e
Filaggrin
×400
f
The average Δ gray-scale intensity of epidermis
*
p=0.03
250
200
150
100
50
0
control
Atg7-/-
g
Involucrin
×400
h
Involucrin
×400
i
The average Δ gray-scale intensity of epidermis
*
p=0.003
250
200
150
100
50
0
control
Atg7-/-
j
LC3
×400
k
LC3
×400
l
The average Δ gray-scale intensity of epidermis
*
p=0.001
250
200
150
100
50
0
control
Atg7-/-

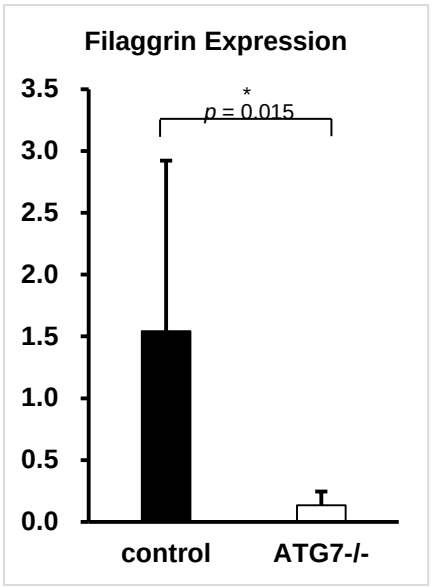
Filaggrin Expression
*
p = 0.015
3.5
3.0
2.5
2.0
1.5
1.0
0.5
0.0
control
ATG7-/-

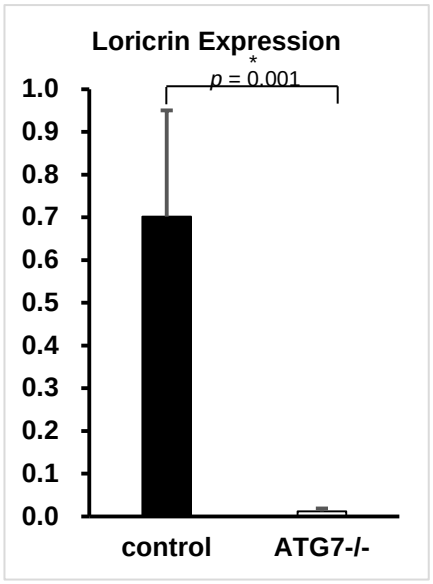
Loricrin Expression
*
p = 0.001
1.0
0.9
0.8
0.7
0.6
0.5
0.4
0.3
0.2
0.1
0.0
control
ATG7-/-

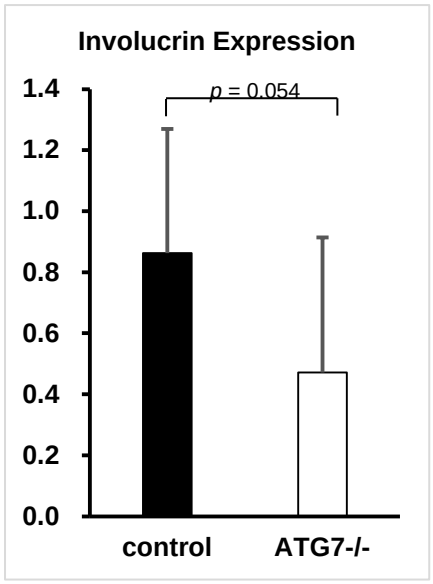
Involucrin Expression
p = 0.054
1.4
1.2
1.0
0.8
0.6
0.4
0.2
0.0
control
ATG7-/-

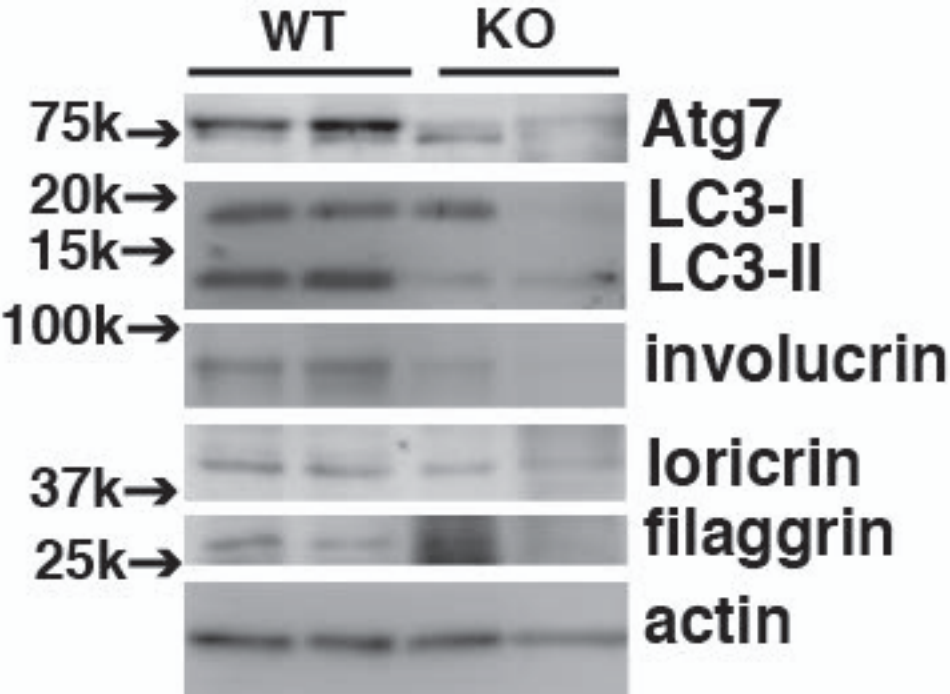
WT
KO
75k→
Atg7
20k→
LC3-I
15k→
LC3-II
100k→
involucrin
loricrin
37k→
filaggrin
25k→
actin

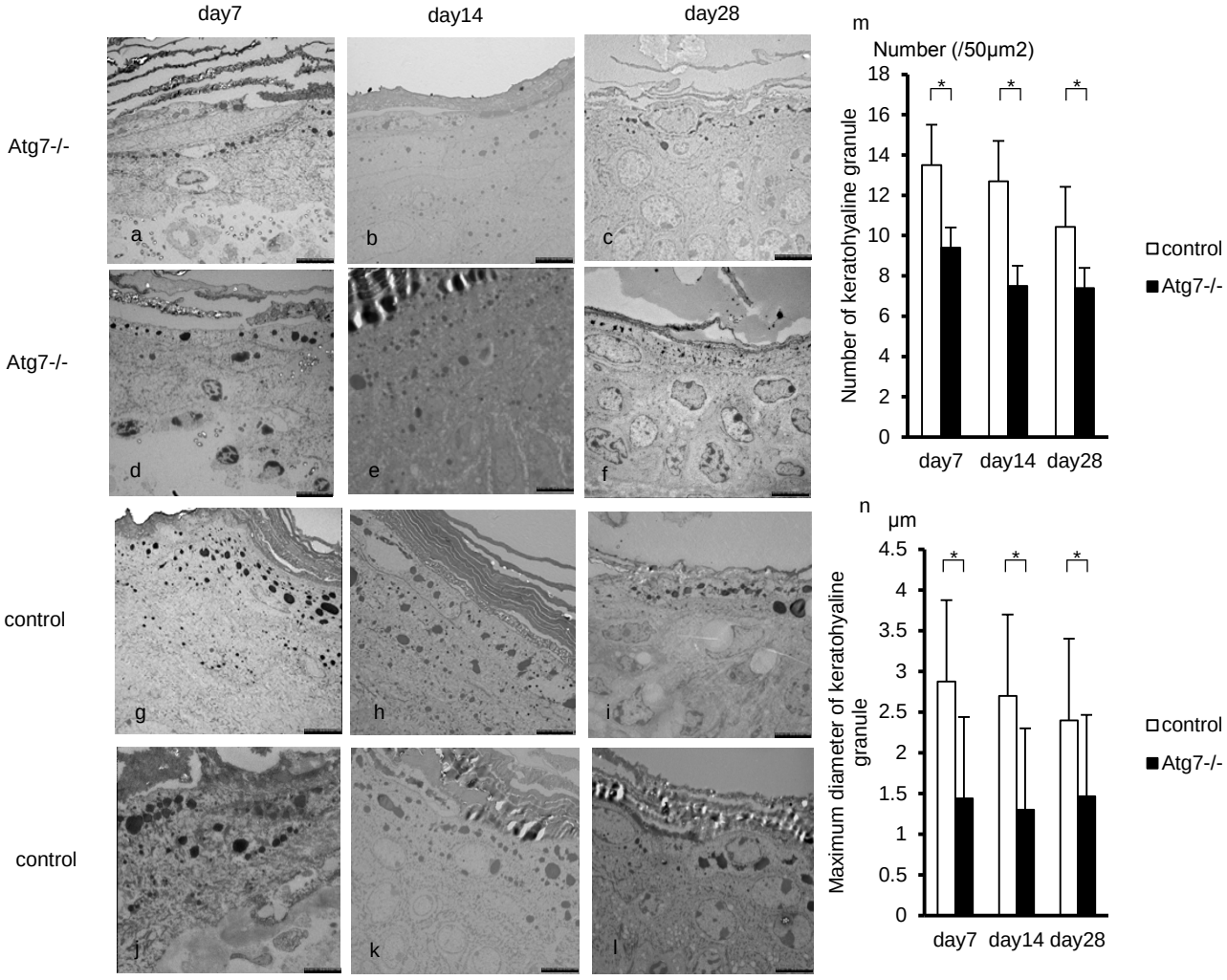
day7
day14
day28
Atg7-/-
Atg7-/-
control
control
a
b
c
d
e
f
g
h
i
j
k
l
m
Number (/50μm2)
Number of keratohyaline granule
18
16
14
12
10
8
6
4
2
0
day7
day14
day28
control
Atg7-/-
n
μm
Maximum diameter of keratohyaline granule
4.5
4
3.5
3
2.5
2
1.5
1
0.5
0
day7
day14
day28
control
Atg7-/-

Atg7-/-

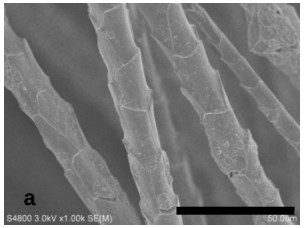

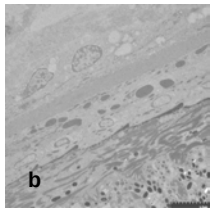

control